



Feasibility Study of Powering Desiccant Evaporative Cooling Systems with Photovoltaic Solar Panels for Hot and Humid Climates of Iran

Ahmad Naderi Nobandegani, Mohammad Ahmadzadehtalatapeh*

Department of Mechanical & Marine Engineering, Chabahar Maritime University, P. O. Box: 99717-56499, Chabahar, Sistan and Baluchestan, Iran.

PAPER INFO
Paper history:

Received 14 April 2020

Accepted in revised form 27 July 2020

Keywords:

 Buildings,
 Energy Consumption,
 Desiccant Evaporative Cooling System (DECS),
 Indoor Air,
 TRNSYS

A B S T R A C T

In the present study, the performance of a Desiccant Evaporative Cooling System (DECS) under eight different designs to provide the desired indoor air conditions for administration buildings was explored via TRNSYS software. An administration building in Chabahar, Iran as a region with a high cooling load demand was considered for the study. The simulation results indicated that the two-stage desiccant cooling system (Des. H) was the most suitable design, and it enjoyed the potential to keep the indoor air conditions within the standard recommendations. It was also shown that Des. H is the superior design in terms of energy performance and can meet the space cooling load requirements. The study showed that Des. H had the highest COP value with 2.83. The possible application of solar energy to the regeneration process of the Des. H was also studied. The simulations revealed that Des. H with and without the solar panels had less energy consumption than the existing system. The study showed that the application of Des. H could ensure 26.97 % saving in power per year in comparison to the existing system. Moreover, it was demonstrated that the addition of PVT panels to Des. H could increase the rate of annual power saving to about 68.03 %.

© 2020 MERC. All rights reserved.

<https://doi.org/10.30501/jree.2020.225286.1096>
1. INTRODUCTION

Energy consumption of air-conditioning systems accounts for a significant part of the world's energy demand, which is about 40 % [1]. High cooling load situations normally coincide with high solar radiation hours, which makes it possible to apply the solar radiation to ventilation systems by related technologies. To this end, Renewable Energy Organization of Iran has recommended a strategic program under the five-year national development vision plan [2]. Based on the proposed plan, Iran is determined to provide 10 % of its electric power demand from renewable resources by 2025 [3].

Solar, wind, biomass, and geothermal energy are considered as the primary sources of renewable energy. Characterized by an average solar radiation 2000 kWh/m^2 with 2800 hours of sunshine per year, which reaches 3200 hours in the central regions of the country, Iran can be considered a rich country in terms of solar energy. Therefore, the application of solar-related technologies has drawn considerable attention by the researchers [4].

The technology of solar-assisted Desiccant Evaporative Cooling System (DECS) is an interesting solution to common issues of buildings. This technology has an open cycle that works based on air dehumidification by solid adsorbent such as silica gel and lithium chloride-cellulose and water evaporation. One of the significant advantages of these systems is the possibility of using solar energy in the recovery line.

The literature review indicates that there are some valuable research studies on the subject [5-10]. For instance, Li et al. [5] examined the performance of a two-stage solar DECS powered by solar energy. It was shown that a two-stage desiccant cooling system could work well for 51 days in an environment that had an average humidity of 51.7 %. A two-stage rotary dehumidification wheel was reviewed by Ge et al. [6]. The primary purpose of this study was to investigate the effect of desiccant thickness on the system performance. It was found that the desiccant with a thickness of 100 mm was the optimal mode for achieving the highest system performance.

Enteria et al. [7] investigated the effect of various adsorbent materials on the performance of a rotary Desiccant Wheel (DW). The performance of two adsorbents including silica gel (SiO_2) and titanium dioxide (TiO_2) was investigated in the study. The results revealed that the application of the titanium dioxide as the moisture absorbent led to better performance. In another research, Liu et al. [8] examined the combination of a DW and a heat pump. In this system, the heat wasted by the gas cooler pump is used to regenerate the DW. The results indicated that the combination saved energy by about 50-90 %.

Preisler et al. [9], and Enteria et al. [7] investigated the performance of flat plate solar collectors to provide the required heat source for the desiccant cooling cycle. In another research, Bourdoukan et al. [10] suggested the application of vacuum tube collectors instead of low-efficiency flat plate collectors in the DECS. The study showed that the fluid output temperature in the vacuum tube collectors was higher than the temperature provided by the flat plates for the regeneration process.

*Corresponding Author's Email: m_ahmadzadeh56@yahoo.com (M. Ahmadzadehtalatapeh)
 URL: http://www.jree.ir/article_111047.html

So far, solar energy has been used in Iran to generate electricity and provide hot water. However, use of solar energy in cooling systems has not received sufficient attention. Therefore, the main objective is to evaluate the performance of the DECS under different designs by replacing this system with the existing operating vapor compression cooling systems in hot and humid regions of Iran. The Chabahar Maritime University Administration Building (CMUAB) is considered as a case study and it is located in the southeast of the country. Of note, the south and southeast of Iran are the areas with high cooling load requirements.

2. RESEARCH METHODOLOGY

The primary purpose of this study is to investigate the potential of replacing the existing ventilation system with a DECS to establish the desired indoor air conditions for an administration building in Chabahar, Iran. For this purpose, first, the existing ventilation system, which is a compression refrigeration type, was simulated by TRNSYS. Then, the existing ventilation system was re-designed to be replaced with a DECS under different designs to determine the most desired configuration in terms of provided indoor air conditions and energy consumption.

3. BUILDING SIMULATION

3.1. Region climate conditions

Chabahar is located on the Makran Coast of the Sistan and Baluchestan province, Iran. It is located in the direction of the Indian subcontinent monsoon wind; therefore, Chabahar

climate is moderate tropical with high Relative Humidity (RH) values [11]. Figure 1 shows the monthly mean ambient RH and temperature for the region.

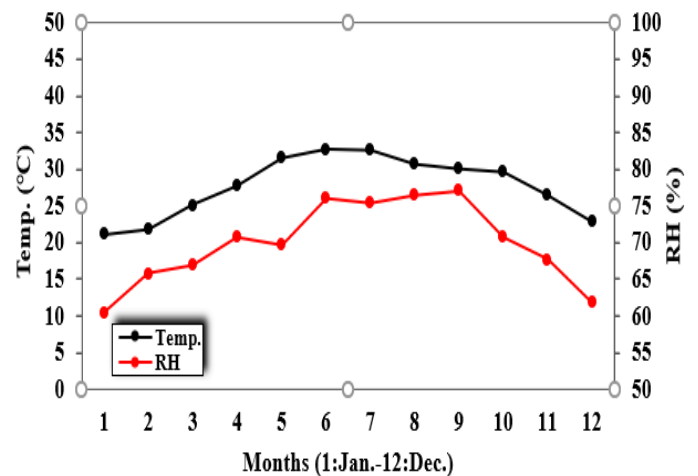


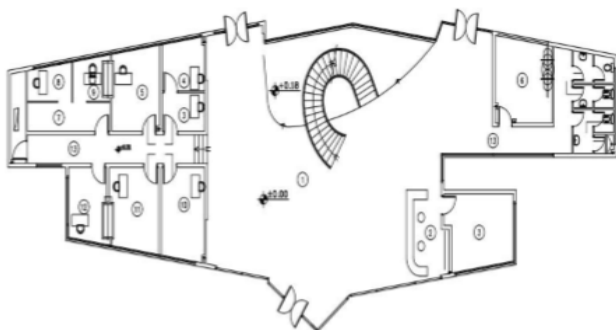
Figure 1. Monthly mean ambient air temperature and RH of the region (Chabahar) [11].

3.2. CMUAB characteristics

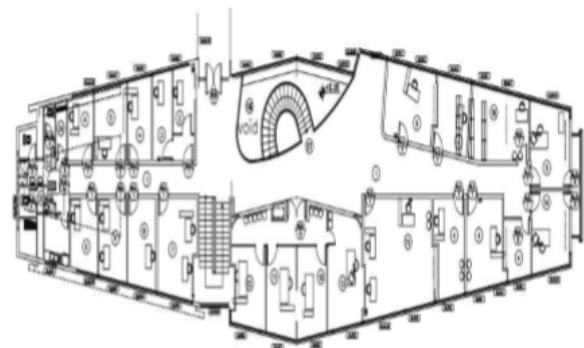
The considered CMUAB is located in Chabahar Maritime University, Chabahar, Iran. The building consists of three separate floors with 51 rooms. The ventilation systems of the floors are the same; however, the cooling capacity of the systems varies for the floors. Figure 2 illustrates the building overview and the plan view of the 1st and 2nd floor.



(a)



(b)



(c)

Figure 2. (a) CMUAB overview, (b) Plan view of the 1st floor, and (c) Plan view of the 2nd floor.

In order to simulate the hourly performance of the considered building under the existing condition and the added DECS, the external walls structure, roof structure, and floor structure need to be determined and defined in the software. Therefore, thickness, material's type, and thermophysical properties of walls were obtained from the

administration department of the CMUAB. Figure 3 demonstrates the walls structure layout and the specifications of the CMUAB elements are tabulated in Table 1.

To determine the indoor air conditions and estimate the required cooling load, the building was simulated in TRNSYS software. The CMUAB was assumed as a single thermal zone

(Type56a), and the required technical data for Type56a were defined. The functions and definitions are tabulated in Table 2.

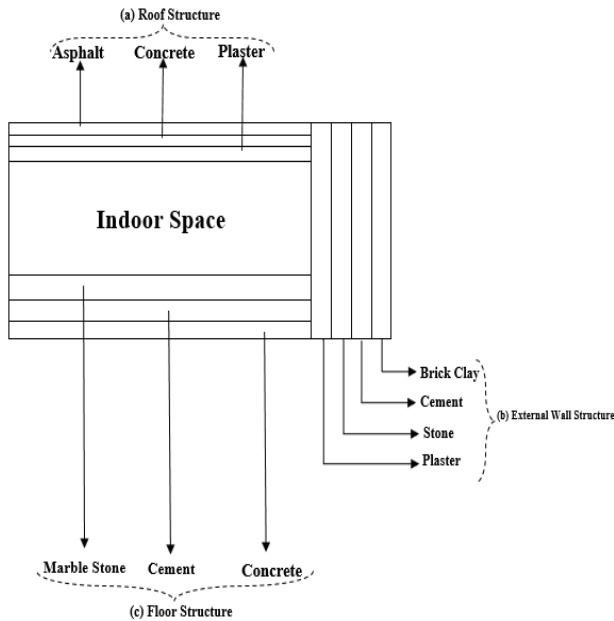


Figure 3. CMUAB roof, external walls, and floor structures layout: (a) Roof structure, (b) External wall structure, (c) Floor structure.

Table 1. Specifications of the CMUAB elements.

Eternal walls				
	d (m)	$\lambda(w/mk)$	$\rho(kg/m^3)$	c (J/kg.k)
Stone	0.015	0.890	1920	790
Cement	0.001	0.580	1900	1000
Brick-Clay	0.20	1.185	2240	790
Plaster	0.015	0.580	800	1090
Floor				
Marble Stone	0.015	0.057	290	590
Cement	0.05	0.580	1900	1000
Concrete	0.30	0.580	1900	1000
Roof				
Asphalt	0.01	0.057	290	590
Concrete	0.30	0.580	1900	1000
Plaster	0.015	0.030	43.0	1210

Table 2. Components definitions (Fig. 7).

Lable	Description of the component	Function
	Equation	This component is used for calculation purposes.
	Region weather data	This component reads TRNSYS TMY2 format weather le to determine the outdoor condition.
	Building (space)	This component takes the inlet temperature, RH, and air flow to calculate the space temperature and RH.
	Ambient related data	This component takes the ambient air data and calculates the fictive sky temperature.
	Thermostat	This component controls the indoor temperature to turn the air conditioning on and off.

	Psychrometric calculator	This component takes any two properties of moist air and calculates all other properties.
	Direct evaporative cooler	This component takes the inlet dry and wet bulb temperatures to calculate the leaving dry and wet bulb temperatures.
	Mixer	Input streamline mixer.
	EW	This component takes the inlet temperature and humidity ratio to calculate the leaving temperature and humidity ratio for the supply and return sides.
	Air heater	This component takes the inlet temperature and humidity ratio to calculate the leaving temperature and humidity ratio.
	Rotary desiccant	This component dries the humid air.
	Photovoltaic thermal collector series	This component generates electricity thermal energy simultaneously

4. CMUAB WITH THE DECS

In this study, different designs based on the DECS principle were investigated. To improve the performance of DECS, some energy converting units such as Direct Evaporative Cooler (DEC), Indirect Evaporative Cooler (IEC), Energy Wheel (EW), DW are normally recommended to be applied to the system. Figures 4 and 5 illustrate the schematic of DW and EW, respectively.

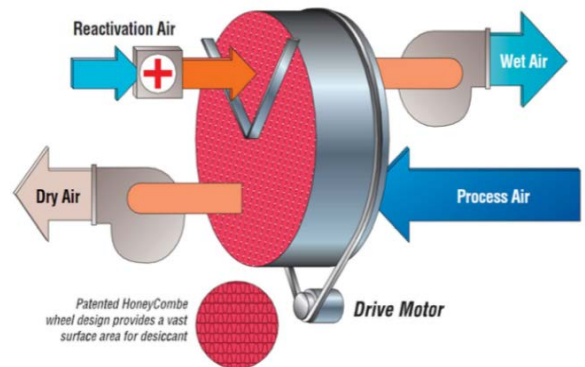


Figure 4. Schematic of a DW [12].

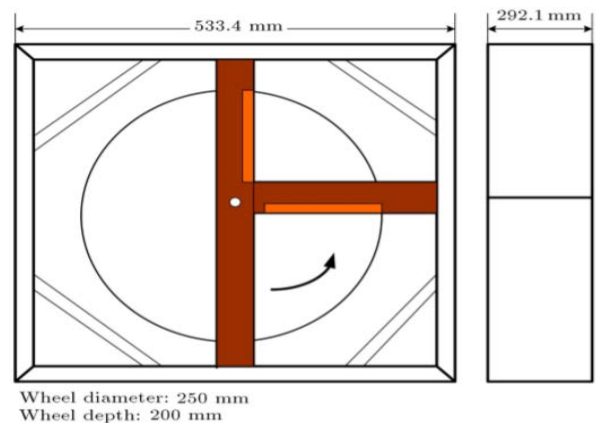


Figure 5. Schematic of an EW [13].

Eight different designs commonly proposed for the Heating, Ventilation, and Air Conditioning (HVAC) systems were examined to determine the most proper design in terms of the established indoor air conditions and energy consumption. The designs are listed below:

1. Des. A: DECS operating in ventilation cycle (Pennington cycle);
2. Des. B: DECS operating in recirculation cycle;
3. Des. C: DECS operating in Dunkle cycle;
4. Des. D: DECS operating in modified ventilation cycle;
5. Des. E: DECS operating in modified recirculation cycle with pre-cooling;
6. Des. F: DECS operating in ventilation cycle with double series EW;
7. Des. G: Two-stage DECS operating in ventilation;
8. Des. H: Two-stage DECS operating in recirculation cycle.

More details regarding the design and simulation process will be explained in the subsections below.

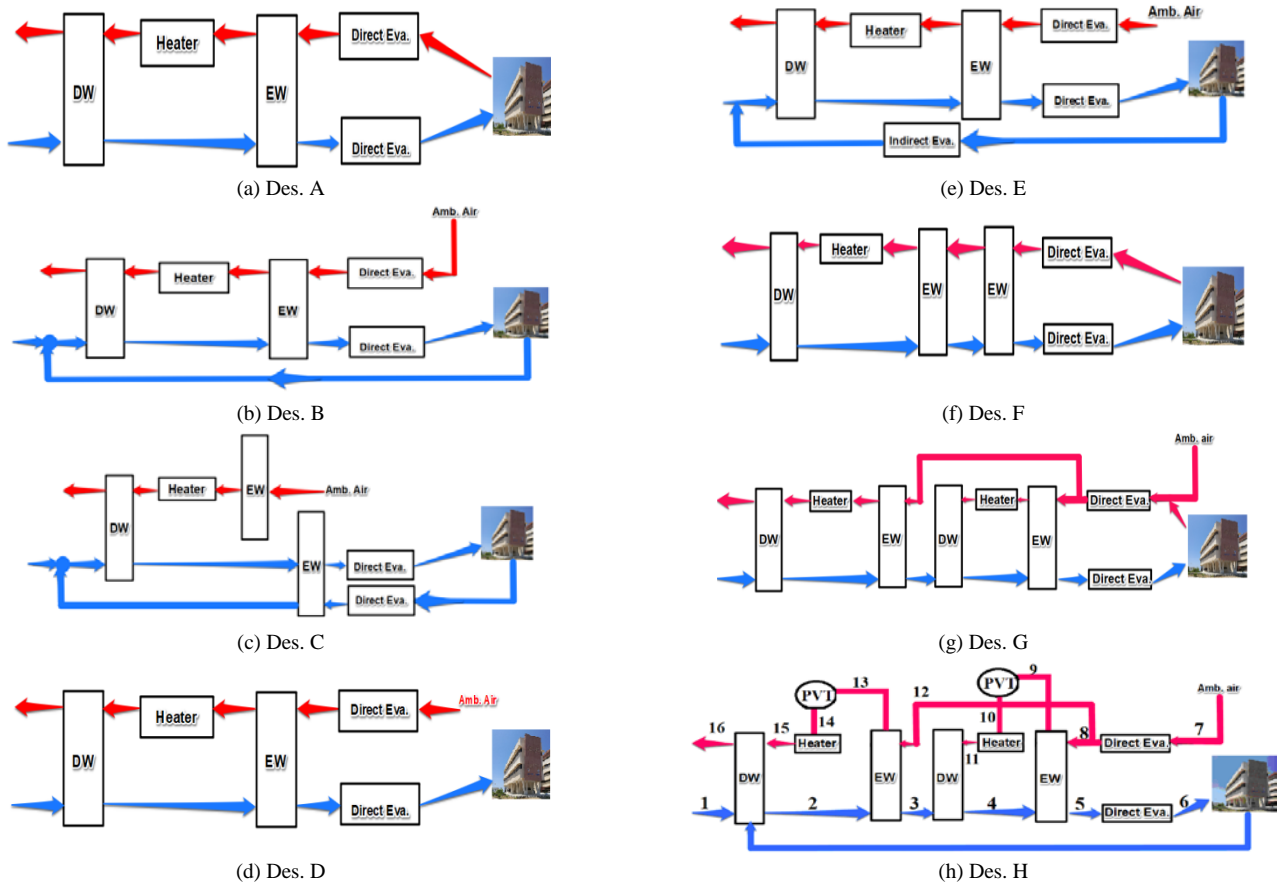


Figure 6. The schematic diagram of desiccant-based cooling systems.

4.2. Des. B: DECS operating in recirculation cycle

To enhance the performance of the Pennington open cycle, some modifications were made to the cycle (Figure 6). In the recirculation cycle, the process air uses the space return air, while the fresh outdoor air is used as the recovery air. Based on the performance principles of the recirculation cycle, using part of the space return air as the supply air reduces the provided air quality, which is the main disadvantage of this design [13].

4.3. Des. C: DECS operating in Dunkle cycle

4.1. Des. A: DECS operating in ventilation cycle (Pennington cycle)

One of the most basic DECS is the Pennington cycle (Figure 6). This cycle consists of two streams of supply and regenerator. In this cycle, fresh outdoor air first passes through a rotary DW and is dehumidified, and its temperature increases. The warm air then passes through an EW and exchanges heat with the recovery stream.

The air after the EW passes through an evaporator unit before entering the building space. The return air from the building is cooled in another evaporator unit directly placed after the building and then, heated by an EW, as shown in Figure 6. Since the regeneration required temperature in DW is about 80-85 °C, air temperature must be sufficiently high enough before entering the DW. Therefore, a heater is typically employed [14].

In this design proposed by Dunkle (Figure 6), a heat exchanger was added to the recirculation cycle to increase the cycle performance [15].

4.4. Des. D: DECS operating in modified ventilation cycle

Des. D is recommended for the applications, where the building's exhaust air is not suitable for the outdoor air co-processing [16]. In this cycle, the ambient air is used in the recovery stream instead of the building's return air (Figure 6). Therefore, the system Coefficient of Performance (COP) value normally is lower than the unmodified system [17].

4.5. Des. E: DECS operating in modified recirculation cycle with pre-cooling

In this design, as illustrated in Figure 6, an IEC was embedded in the cycle to increase the cooling capacity. The IEC cools the air passing through, before entering the DW. In this process, the ambient air is used as the regeneration air [18].

4.6. Des. F: DECS operating in ventilation cycle equipped with double series EW

EW thermal efficiency has a significant impact on the performance of the ventilation cycle. In this design, an extra EW was added to the ventilation cycle to achieve a possible improvement in the cooling capacity of the system [13]. In this design, the supply air passes through the rotary DW, two EWs, and a DEC before entering the space (Figure 6).

4.7. Des. G: Two-stage DECS operating in ventilation cycle

Des. G was proposed by Sopian et al. [18] to enhance cooling capacity and performance of the desiccant system. This design employs two rotary DWs, two EWs, and a direct evaporator in the supply air stream. Besides, in the regeneration line, two EWs, two rotary DWs, and one DEC are used (Figure 6).

4.8. Des. H: Two-stage DECS operating in recirculation cycle

Sopian et al. [18] also proposed Des. H, as a modified version of Des (Figure 6). Adding part of exhaust air from the building to the supply stream and using the ambient air in the regeneration line are the two significant modifications in this cycle. Fig. 7 represents the simulated layout of Des. H.

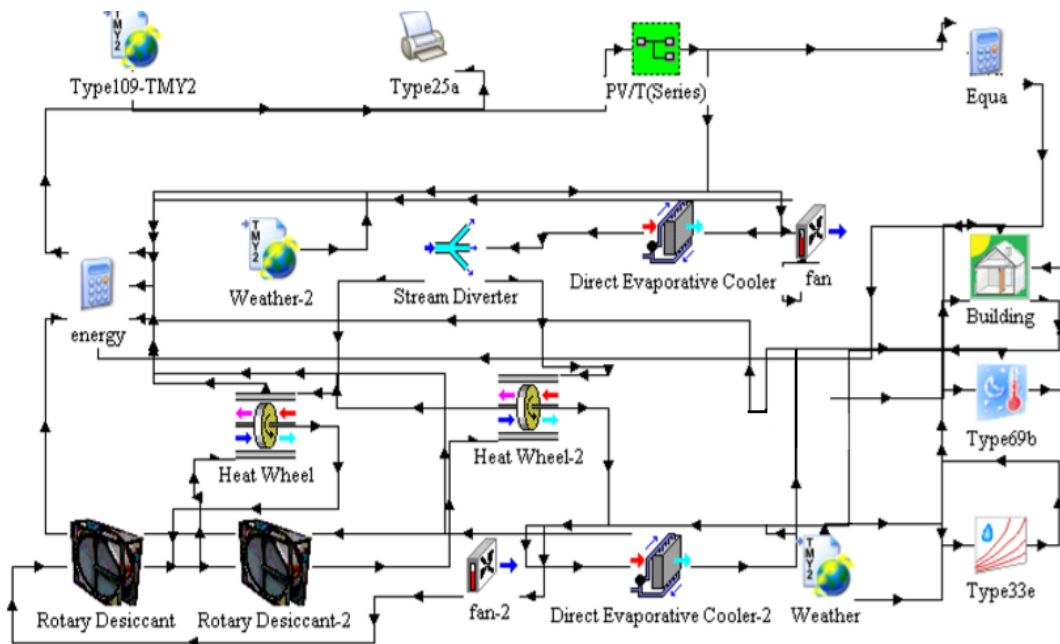


Figure 7. Simulation layout of Des. H in TRNSYS software.

4.9. Building existing HVAC system

The existing HVAC system operating in the building is a simple compression cycle. Three Air Handling Units (AHU) with cooling capacities of 700, 1000, and 1300 were employed for the building. In order to simulate the AHUs in TRNSYS, the mathematical performance of the AHUs was extracted from the AHUs manuals. The mathematical equations were written in FORTRAN source codes and were added to the software library to be used as a user-defined component for the simulation process.

5. FEASIBILITY OF USING SOLAR ENERGY IN THE DECS

One of the most essential advantages of the DECS cycle is the possibility of using solar energy in the regeneration streamline. Therefore, in this study, the feasibility of providing thermal and electrical energy by the Photovoltaic Thermal collectors (PVT) was also explored. Prior to the feasibility study, the solar radiation potential of the region was evaluated. TMY data for the region were used for this purpose (Table 3). According to Table 3, the application of PVT panels is justified [19].

Table 3. Monthly mean and maximum solar radiation potential of Chabahar.

Months	Mean. rad.	Max. rad.
	kJh/m^2	kJh/m^2
Jan.	2434.36	4109.01
Feb.	2845.16	4538.88
Mar.	3478.87	6148.55
Apr.	3800.72	7025.88
May	4308.42	7297.54
Jun.	4347.54	8386.38
Jul.	4101.90	8062.46
Aug.	3942.44	7659.19
Sep.	3627.56	6631.41
Oct.	3305.17	5163.19
Nov.	2818.02	4476.91
Dec.	2250.72	3928.05

Due to the space constraints on the building roof, the maximum number of 40 PVT panels can be installed. In addition, in order to install PVT panels, the latitude and longitude of the building site and the angle of the PVT panels need to be determined. It is clear that the optimum angle reduces the system waste and increases energy production. It was found that the optimum angle of the panels was about 27 degrees, as shown in Figure 8.

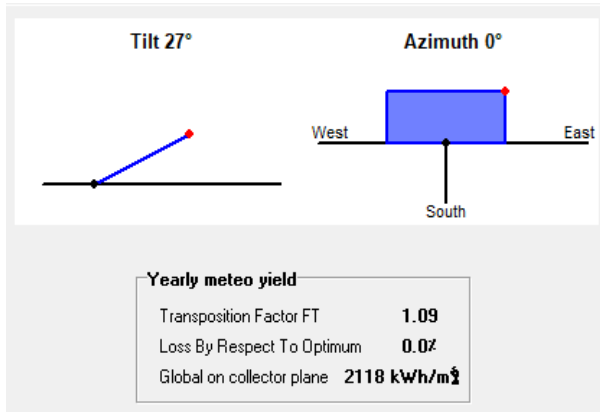


Figure 8. The optimum angle of the PVT panels.

In order to optimize the arrangement of PVT panels, PVSYS software was employed. Based on the shadow tests conducted by the software, the sun has the most significant amount of radiation between 9:00 and 15:00 hours of a day; thus, the absence of shade on the panels is necessary at these hours. Therefore, the arrangement of the PVT panels in the four-row form was recommended. Figure 9 shows the arrangement of PVT panels on the CMUAB roof.

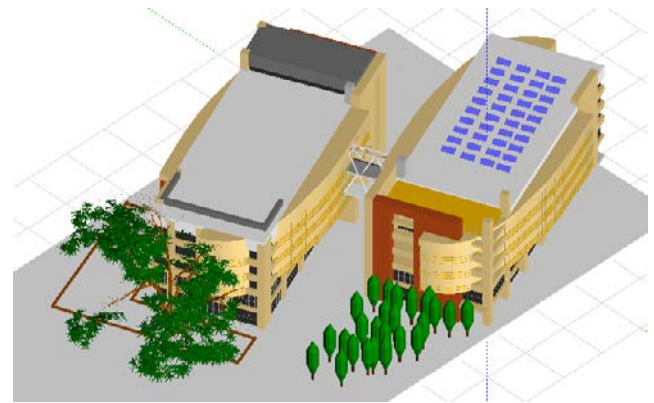


Figure 9. CMUAB with PVT panels.

5.1. Solar collectors simulation results

As already mentioned above, one of the interesting characteristics of the DECS is the possibility of providing the desiccant required regeneration heat energy by renewable resources such as solar energy. In this section, the potential of airflow temperature being provided by different collectors, namely, G-BIPC, ETC, LPCC, PV-T, UTC, UAHC, and UBIP, was evaluated to determine the most desired collector for the application in DECS. To this end, the panels were considered in the two-row form to measure the temperature of the air passing through the panels. It should be noted that the air is driven through the panels by the fans. The study revealed that the panels are capable of providing the mean temperature values of 24.3 °C 44.41 °C 53.5 °C 41.3 °C 45.6 °C 43.1 °C and 42.4 °C for the air passing through for the G-BIPC, ETC, LPCC, PVT, UTC, UAHC, and UBIP panels, respectively (see Figure 10).

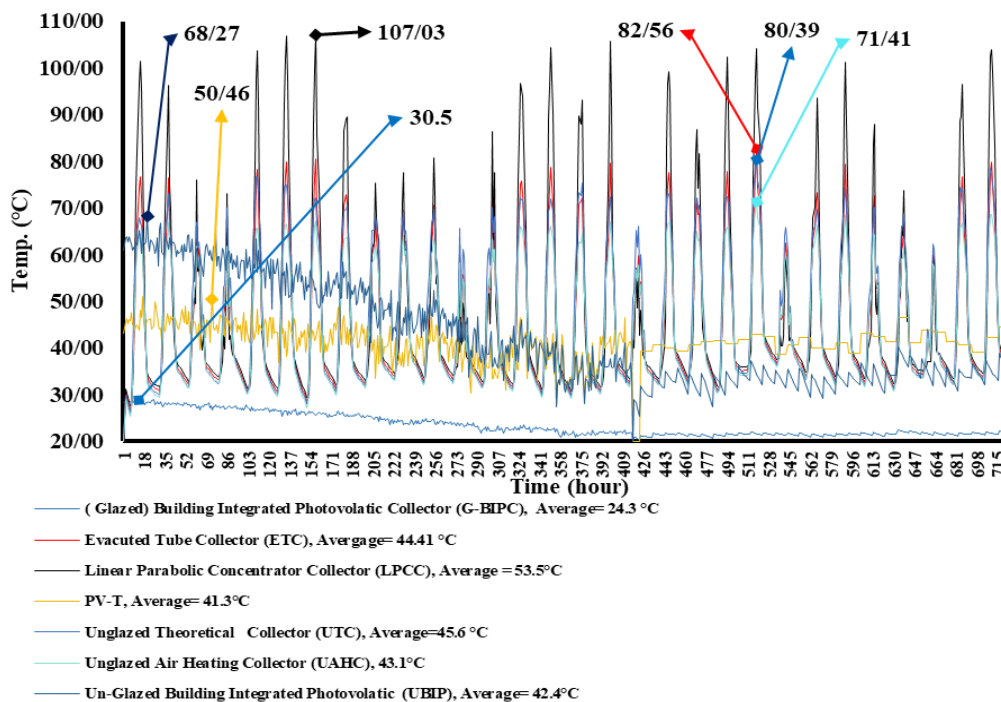


Figure 10. Airflow temperature provided by the solar panels.

5.2. Photovoltaic thermal collectors (PVT)

Performance analysis indicates that for the present study, which is an energy-related case, the PVT panels are more desired than the solar thermal collectors, because PVT panels have the dual purpose of providing electrical energy by the PV

cells and establishing a source of heat energy for possible low-grade temperature applications such as the DECS regeneration process.

This is achieved by the waste heat rejected into the air stream passing through the PVT panels, as illustrated in

Figure 11. In addition, heat rejection is useful for cooling the PV cells allowing higher power conversion efficiencies. Therefore, PVT panels are recommended for DECS application purposes in the present research.

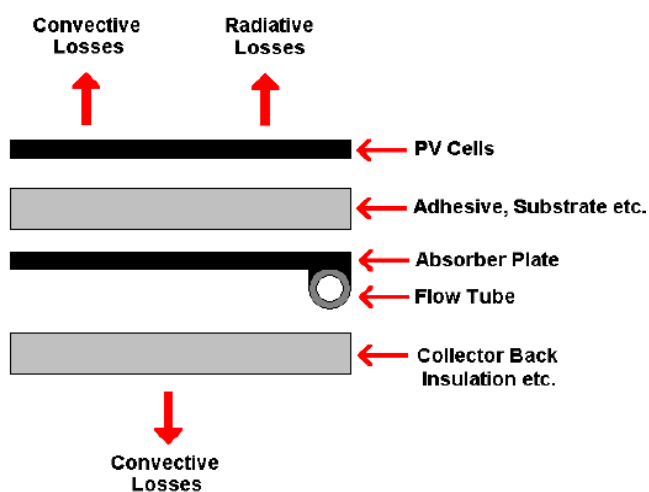


Figure 11. PVT panels layers.

In order to define the PVT as a component in the TRNSYS library, the mathematical performance of the PVT panels was needed to be employed.

The efficiency of the PV cells is a function of the cell temperature and the incident solar radiation, as given by the following equation:

$$\eta_{PV} = \eta_{Nominal} \times X_{Cell.Temp} \times X_{Rad} \quad (1)$$

where:

$$X_{Cell.Temp} = 1 + Eff_T (T_{PV} - T_{ref}) \quad (2)$$

and

$$X_{Rad} = 1 + Eff_G (G_T - G_{ref}) \quad (3)$$

The collector's useful energy gain can now be calculated:

$$Q_u = \dot{m}C_p (T_{Fluid,out} - T_{Fluid,in}) \quad (4)$$

Moreover, the collector's useful energy gain per unit length can be calculated as:

$$Q' = Q'_{Fluid} = (\dot{m}C_p (T_{Fluid,out} - T_{Fluid,in})) / LN_{tube} \quad (5)$$

The above mathematical performance equations were written using a FORTRAN source code to define the PVT as a component so that it can be used in TRNSYS studio.

6. SIMULATION RESULTS FOR THE BUILDING WITHOUT HVAC SYSTEM

In order to estimate the performance of the examined DECS on the building, the indoor air conditions without any cooling system (building without the HVAC system) need to be determined at the first phase of the study.

Then, possible improvements to the established indoor air conditions with the help of added DECS should be investigated. The simulation results of the indoor air conditions for the case of building without the HVAC system are tabulated in Table 4. In Table 4, the monthly meant indoor air temperature and RH are tabulated.

Table 4. Monthly mean indoor air temperature and indoor RH of the CMUAB (Building without HVAC).

Month	I.T. (°C)	LRH (%)
Jan.	21.8	56.0
Feb.	22.7	57.3
Mar.	26.9	54.4
Apr.	28.3	48.0
May	33.3	41.2
Jun.	33.7	57.2
Jul.	33.9	68.1
Aug.	33.0	70.9
Sep.	32.1	66.7
Oct.	31.1	53.9
Nov.	26.8	57.1
Dec.	23.7	58.5

The simulation values were compared with the field measurements. The comparison shows less than 10 % deviation between the simulation results and fieldwork measurements. To determine the months in which the building requires the cooling load, the data tabulated in Table 4 were compared with the standard recommendations for thermal comfort, i.e., (20 °C-26.5 °C) and (45 %-65 %) [20]. These months were considered for further simulations by the DECS added to the building.

7. SIMULATION RESULTS OF THE BUILDING WITH THE ADDED DECS

7.1. Established indoor air conditions

Table 5 shows the mean indoor air and RH values established by the studied DECS designs added to the building. As explained above in the paper, the months which require cooling load were only considered for the simulations. For instance, as tabulated in Table 5, Des. A is only capable of providing standard indoor air conditions for March, April, May, June, and November. However, it does not have the potential to meet the standard indoor air conditions for July, August, September, and October. Figure 12 illustrates the established indoor air temperature in March until November (the months which require cooling load, Table 4) for the CMUAB without the HVAC system and CMUAB under Des. F to graphically compare the outcomes of adding Des. F as a representative of the configurations examined. However, for simplicity, all of the simulated values are tabulated in Table 5. The simulation indicated that Des. F is capable of providing mean values of 27.7 °C, 28.1 °C, 28.1 °C, and 27.5 °C for July, August, September, and October, respectively. The mean indoor air temperature at the working hours is also illustrated for a typical day in July by Des. F and Des. H in Figures 13 and 14, respectively, as the representative of the designs examined. According to the simulated values in Table 5, Des. G and Des. H have the capability to establish the desired indoor air conditions in the space in terms of indoor air temperature; however, Des. H has the potential to provide both of the temperature and RH values within the range recommended by the standards. Therefore, Des. H is the most

proper design and is recommended to be applied to the building. Des. H is capable of establishing the indoor air temperatures at 20.9 °C, 20.7 °C, 21.6 °C, 23.5 °C, 25.3 °C,

25.6 °C, 25.7 °C, 25 °C, and 23.8 °C in March, April, May, June, July, August, September, October, and November, respectively.

Table 5. Provided indoor air conditions by DECS designs (mean values).

Configs.		Months								
		Mar.	Apr.	May	Jun.	Jul.	Aug.	Sep.	Oct.	Nov.
Des. A	I.T. (°C)	22.8	22.3	23.5	25.6	27.5	27.9	27.9	27.2	26.0
	R.H. (%)	56.8	57.6	55.7	52.2	48.7	48.3	48.3	49.1	51.1
Des. B	I.T. (°C)	59.4	60.2	61.1	60.9	59.4	60.8	61.0	59.6	58.4
	R.H. (%)	23.2	22.5	24.2	26.6	29.0	29.6	29.7	28.8	27.0
Des. C	I.T. (°C)	64.8	65.9	66.2	65.2	64.0	65.2	65.5	64.4	63.5
	R.H. (%)	23.6	22.8	24.5	26.9	29.3	29.9	30.1	29.2	27.4
Des. D	I.T.(°C)	22.5	24.2	26.5	28.9	29.6	29.7	28.8	27.1	23.3
	R.H. (%)	59.4	60.2	61.1	60.7	59.2	60.5	60.7	59.4	58.3
Des. E	I.T. (°C)	22.4	21.8	23.4	25.8	28.1	28.7	28.9	27.9	26.2
	R.H. (%)	55.1	55.6	56.8	56.7	55.5	57.0	57.2	55.7	54.4
Des. F	I.T. (°C)	23.0	22.5	23.7	25.8	27.7	28.1	28.1	27.5	25.2
	R.H. (%)	59.0	59.9	58.0	54.5	51.1	50.7	50.7	51.5	53.5
Des. G	I.T. (°C)	24.7	20.2	21.1	23.1	25.0	25.4	25.4	23.4	20.4
	R.H. (%)	55.6	57.5	54.8	51.0	48.6	48.4	48.5	49.1	50.6
Des. H	I.T. (°C)	20.9	20.7	21.6	23.5	25.3	25.6	25.7	25.0	23.8
	R.H. (%)	58.7	59.0	57.6	53.8	50.4	50.1	50.1	51.0	52.8

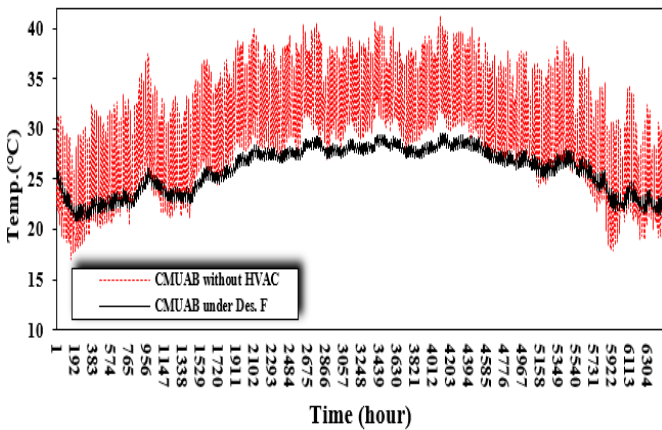


Figure 12. Hourly simulation responses of the existing space without DECS and existing space under Des. F in March until November.

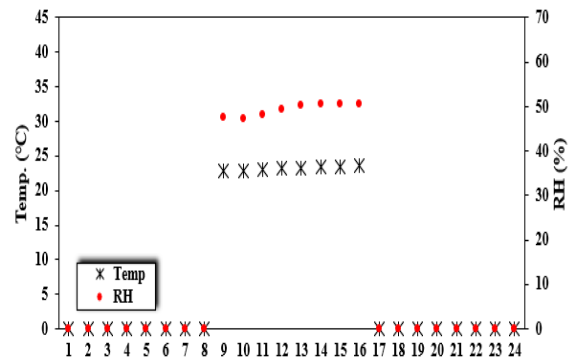


Figure 14. Hourly simulated indoor air conditions within eight working hours (8:00 am till 15:00 pm) for a typical day in July by Des. H.

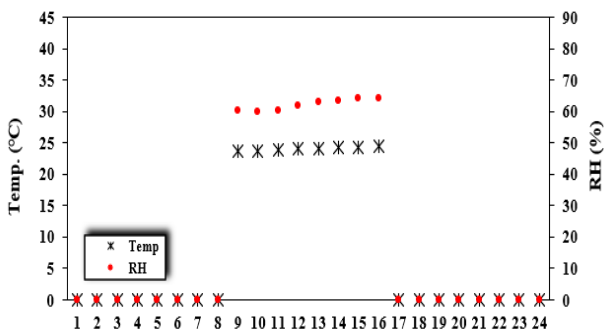


Figure 13. Hourly simulated indoor air conditions within eight working hours (8:00 am till 15:00 pm) for a typical day in July by Des. F.

In Des. H, a fraction of indoor air (Bypass) is mixed with the fresh outdoor air and enters the first DW (latent wheel) unit which absorbs the moisture contents of the income air; therefore, the air temperature increases (temperature from 30.42 °C to 40.31 °C and humidity ratio from 0.02122 to 0.00963). Then, the DW leaving hot and dry air passes through the first EW unit (as the sensible heat transfer unit) to exchange heat with the regeneration line (temperature from 40.31 °C to 32.45 °C and humidity ratio remaining constant as 0.00963). In the next process, the air is further dehumidified by the second DW unit (temperature from 32.45 °C to 42.50 °C and humidity ratio from 0.00963 to 0.00835) and enters the second EW unit for the heat exchange with the return flow line (temperature from 42.50 °C to 33.43 °C and

humidity ratio remaining constant as 0.00835). The established air conditions by the units are outside the ASHRAE recommended standards scope; therefore, a DEC was employed before the building (temperature from 33.43 °C to 18.24 °C and humidity ratio of 0.00835 to 0.0112). The return flow line is divided into two branches and the return air passes through the same energy units. In order to provide a higher temperature gradient in the EW units, the air passes

through the DEC first. In this line, thermal solar panels are planned to be used for reducing energy consumption. The Des. H air processes in the psychrometric diagram are shown in Figure 15. Keeping the above mind, in Des. H, division of the air into two branches on the way back and the presence of bypass line have increased the design efficiency and improved the air quality of the indoor air compared to the other examined designs.

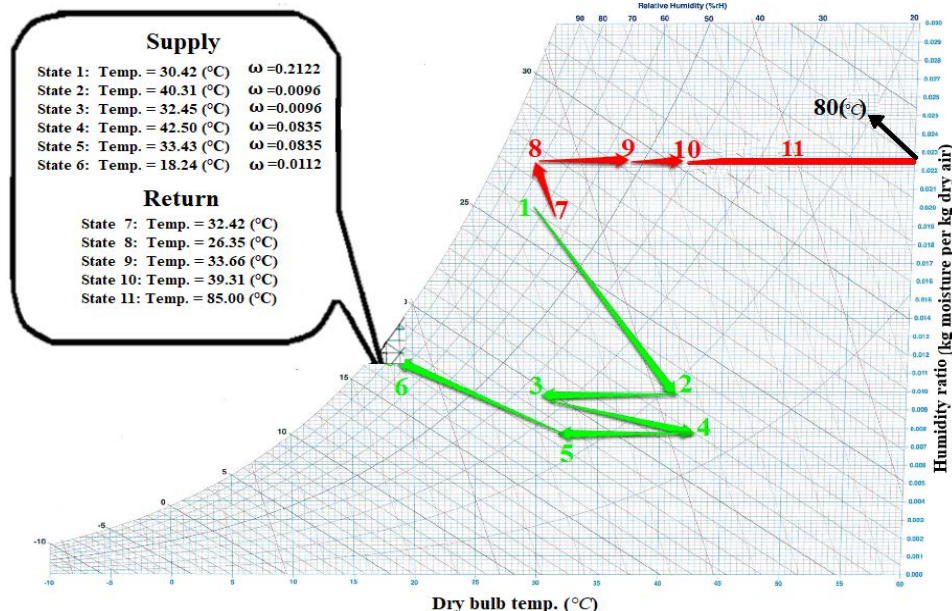


Figure 15. Air process under the Des. H in the psychrometric diagram for typical July.

7.2. COP analysis

As explained above, the Des. H has the most desired performance in terms of provided indoor air conditions. Therefore, the COP value for this design was also explored for the studied months of the year. The COP value is defined as the ratio of heat taken to the heat required. The heat taken is the amount of cooling load applied to the building by the supply streamline. Therefore, the COP value for Des. H as the two-stage DECS under the recirculation mode could be written as follows [5]:

$$COP = \dot{m}_s (h_1 - h_6) / \dot{m}_r (h_{12} - h_{11}) + \dot{m}_r (h_{15} - h_{14}) \tag{6}$$

The COP values for the Des. H in the studied months were determined, as shown in Table 6.

Table 6. The COP values for the Des. H.

Months	COP value
Mar.	2.82
Apr.	1.42
May	1.36
Jun.	1.52
Jul.	1.62
Aug.	1.40
Sep.	1.50
Oct.	0.98
Nov.	1.98

The following equation is used to calculate the COP of other studied designs [5]:

$$COP = \Delta h_s / \Delta h_r \tag{7}$$

The COP for the examined designs was determined for typical March, as the representative of the months of the year. As illustrated in Figure 16, Des. H has the highest COP value at 2.83.

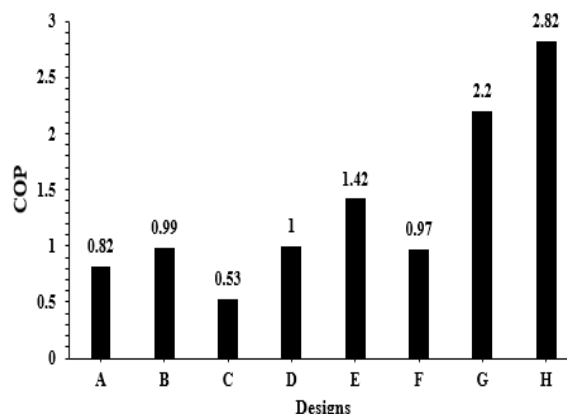


Figure 16. COP value for designs (A-H) for typical March.

8. POWER CONSUMPTION BY Des. H

The power consumption of the building for the existing system, Des. H, and Des. H with the PVT is evaluated in this section. Figure 17 shows hour-by-hour power consumption by the Des. H for typical July. As illustrated in Figure 18, about 50.34 % savings in Des. H could be achieved by the application of PVT application. The study showed that the

application of Des. H, would ensure 26.97 % power saving per year, compared to the existing system. Moreover, it was proved that the yearly saving could be increased to about 68.03 % by adding PVT panels to Des. H.

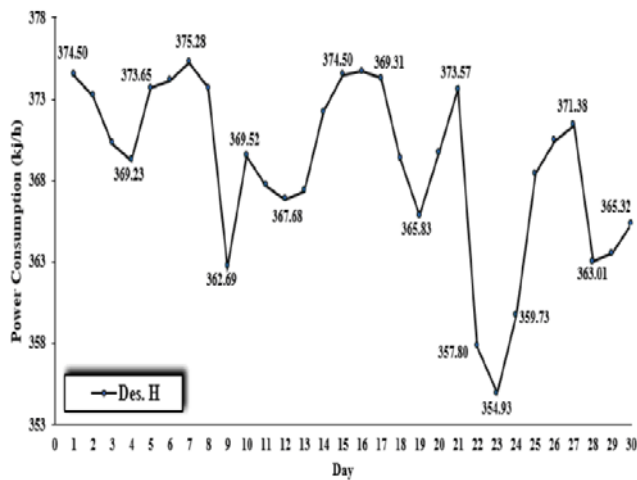


Figure 17. Hour-by-hour power consumption by Des. H for typical July.

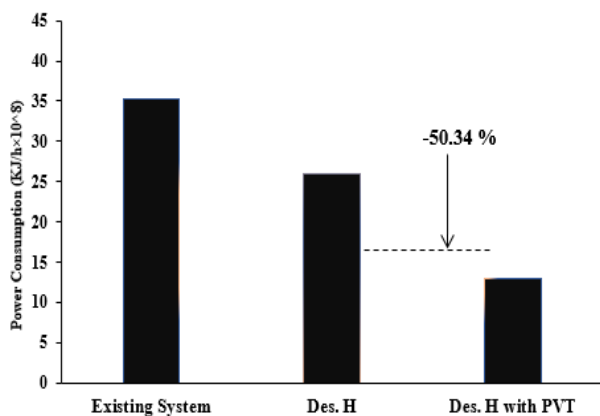


Figure 18. Power consumption by the existing system, Des. H and Des. H with the added PVT.

9. CONCLUSIONS

The present study investigated the feasibility of solar-assisted DECS for buildings located in the high cooling load required region of Iran. To this end, the administration building in Chabahar Maritime University, Chabahar, Iran (CMUAB) was considered. In the first phase of the research, the CMUAB was simulated under the existing cooling system. Then, the feasibility of replacing the existing cooling system with solar DECS was explored. Eight different designs based on DECS were examined in terms of the provided indoor air conditions and energy performance to determine the most proper design for the building. The existing system and the building integrated with the DECS were studied for the whole year of operation. TRNSYS software was employed for this purpose, and the TMY weather data for the region were used as the input file for the program. Based on the simulation data, Des. H, as the two-stage DECS, had the potential to provide the required indoor air conditions for the studied months of the year. It was also found that Des. H had the highest COP value at 2.83 in March as the representative of the months examined.

The application of solar energy to the regeneration process in the Des. H was also explored. It was found that Des. H with

and without the PVT had lower energy consumption than the existing ventilation system. It was also found that the application of Des. H ensured 26.97 % power saving per year, compared to the existing system. Moreover, it was shown that Des. H could reduce power consumption by about 68.03 % by adding the PVT panels.

10. ACKNOWLEDGEMENT

The authors would like to acknowledge the financial assistance from the Chabahar Maritime University, Iran to the authors to conduct the research.

NOMENCLATURE

C	Heat capacity (kj/s.k)
Cp	Specific heat (kJ/Kg.k)
d	Materials thickness (m)
Eff	Efficiency
FT	Transposition factor
G	Radiation (KJ/m ² .h)
h	Enthalpy
L	Collector tube length (m)
m	Mass flow rate (Kg/h)
QU	Useful energy delivered by collector (Kj/h)
Q'	collector useful energy gain per unit length
X _{Cell.Temp}	Multiplier for the PV cell efficiency as a function of the cell temperature
X _{Rad}	Multiplier for the PV cell efficiency as a function of the incident radiation

Greek letters

η	Efficiency
λ	Heat conductivity
ρ	Density of a Material
Δ	Gradient
ω	Absolute ratio

Subscripts

Fluid,in	Inlet fluid (kg/h)
Fluid,out	Outlet fluid (kg/h)
Nominal	Refers to the reference conditions
r	Regeneration streamline
Rad	Sun radiation
ref	Reference ambient (°C)
s	Supply streamline

Abbreviations

AHU	Air handling unit
Amb	Ambient
ASHRAE	American society of heating, refrigerating and air conditioning engineers
CMUAB	Chabahar maritime university administration building
COP	Coefficient of performance
DECS	Desiccant based evaporative cooling system
Des	Design
DW	Desiccant wheel
DEC	Direct evaporator cooler
Eva	Evaporator
ETC	Evacuated tube collector
EW	Energy wheel
G-BIPS	(Glazed) building integrated photovoltaic collector
HVAC	Heating, ventilation, and air conditioning
IEC	Indirect evaporative cooler
IRH	Indoor relative humidity
I.T	Indoor temperature
LDCS	liquid desiccant cooling system
LPCC	Linear parabolic concentrator collector

N _{Tube}	Number of tube
PVT	Photovoltaic thermal collector
RH	Relative humidity
SDCS	Solid desiccant cooling system
Temp	Temperature
TMY	Typical meteorological year
TRNSYS	Transient system simulation software
UAHC	Unglazed air heating collector
UBIP	Un-glazed building integrated photovoltaic
UTC	Unglazed theoretical collector

Vol. 30, (2012), 668-675.
(<https://doi.org/10.1016/j.egypro.2012.11.076>).

10. Bourdoukan, P., Wurtz, E., Joubert, P. and Sperandio, M., "Potential of solar heat pipe vacuum collectors in the desiccant cooling process: Modelling and experimental results", *Solar Energy*, Vol. 82, No. 12, (2008), 1209-1219. (<https://doi.org/10.1016/j.solener.2008.06.003>).
11. Ahmadzadehtalatapeh, M. and Khaki, S., "Application of phase change material (PCM) for cooling load reduction in lightweight and heavyweight buildings: Case study of a high cooling load region of Iran", *Journal of Renewable Energy and Environment (JREE)*, Vol. 5, No. 2, (2018), 31-40. (<https://doi.org/10.30501/jree.2018.88632>).
12. Nie, J., Fang, L., Zhang, G., Sheng, Y., Kong, X., Zhang, Y. and Olesen, B.W., "Theoretical study on volatile organic compound removal and energy performance of a novel heat pump assisted solid desiccant cooling system", *Building and Environment*, Vol. 85, (2015), 233-242. (<https://doi.org/10.1016/j.buildenv.2014.11.034>).
13. Ahmadzadehtalatapeh, M., "Solar assisted desiccant evaporative cooling system for office buildings in Iran: A yearly simulation model", *Scientia Iranica*, Vol. 25, No. 1, (2018), 280-298. (<https://doi.org/10.24200/SCI.2017.4323>).
14. Ge, T.S., Li, Y., Wang, R.Z. and Dai, Y.J., "A review of the mathematical models for predicting rotary desiccant wheel", *Renewable and Sustainable Energy Reviews*, Vol. 12, No. 6, (2008), 1485-1528. (<https://doi.org/10.1016/j.rser.2007.01.012>).
15. Pridasawas, W., "Solar-driven refrigeration systems with focus on the ejector cycle", Ph.D. Thesis, Royal Institute of Technology, KTH, Stockholm, (2006).
16. La, D., Dai, Y.J., Li, Y., Wang, R.Z. and Ge, T.S., "Technical development of rotary desiccant dehumidification and air conditioning: A review", *Renewable and Sustainable Energy Reviews*, Vol. 14, No. 1, (2010), 130-147. (<https://doi.org/10.1016/j.rser.2009.07.016>).
17. Rafique, M.M., Gandhidasan, P., Rehman, S. and Al-Hadhrani, L.M., "A review on desiccant based evaporative cooling systems", *Renewable and Sustainable Energy Reviews*, Vol. 45, (2015), 145-159. (<https://doi.org/10.1016/j.rser.2015.01.051>).
18. Sopian, K., Dezfouli, M.M.S., Mat, S. and Ruslan, M.H., "Solar assisted desiccant air conditioning system for hot and humid areas", *International Journal of Environment and Sustainability*, Vol. 3, No. 1, (2014). (<https://doi.org/10.24102/ijes.v3i1.447>).
19. Keshavarz, S.A., Talebizadeh, P., Adalati, S., Mehrabian, M.A. and Abdolzadeh, M., "Optimal slope-angles to determine maximum solar energy gain for solar collectors used in Iran", *International Journal of Renewable Energy Research*, Vol. 2, No. 4, (2012), 665-673. (<https://ijrer.org/ijrer/index.php/ijrer/article/view/367>).
20. ASHRAE, ASHRAE Standard 62.1-2016, Atlanta, USA, (2016).

REFERENCES

1. Karbassi, A.R., Abdul, M.A. and Mahin Abdollahzadeh, E., "Sustainability of energy production and use in Iran", *Energy Policy*, Vol. 35, No. 10, (2007), 5171-5180. (<https://doi.org/10.1016/j.enpol.2007.04.031>).
2. Ghobadian, B., Najafi, G., Rahimi, H. and Yusaf, T.F., "Future of renewable energies in Iran", *Renewable and Sustainable Energy Reviews*, Vol. 13, No. 3, (2009), 689-695. (<https://doi.org/10.1016/j.rser.2007.11.010>).
3. Fadaei, D., Shams Esfandabadi, Z. and Abbasi, A., "Analyzing the causes of non-development of renewable energy-related industries in Iran", *Renewable and Sustainable Energy Reviews*, Vol. 15, No. 6, (2011), 2690-2695. (<https://doi.org/10.1016/j.rser.2011.03.001>).
4. Hosseini, S.E., Mohammadzadeh Andwari, A., Abdul Wahid, M. and Bagheri, G., "A Review on green energy potentials in Iran", *Renewable and Sustainable Energy Reviews*, Vol. 27, (2013), 533-545. (<https://doi.org/10.1016/j.rser.2013.07.015>).
5. Li, H., Dai, Y.J., Köhler, M. and Wang, R.Z., "Simulation and parameter analysis of a two-stage desiccant cooling/heating system driven by solar air collectors", *Energy Conversion and Management*, Vol. 67, (2013), 309-317. (<https://doi.org/10.1016/j.enconman.2012.11.005>).
6. Ge, T.S., Dai, Y.J. and Wang, Y.L., "Performance of two-stage rotary desiccant cooling system with different regeneration temperatures", *Energy*, Vol. 80, (2015), 556-566. (<https://doi.org/10.1016/j.energy.2014.12.010>).
7. Enteria, N., Yoshino, H., Satake, A., Mochida, A., Takaki, R., Yoshie, R., Mitamura, T. and Baba, S., "Experimental heat and mass transfer of the separated and coupled rotating desiccant wheel and heat wheel", *Experimental Thermal and Fluid Science*, Vol. 34, No. 5, (2010), 603-615. (<https://doi.org/10.1016/j.expthermflusci.2009.12.001>).
8. Liu, Y., Meng, D. and Sun, Y., "Feasible study on desiccant wheel with CO₂ heat pump", *Proceedings of IOP Conference Series: Earth and Environmental Science*, Vol. 100, No. 1, (2017), 012209. (<https://doi.org/10.1088/1755-1315/100/1/012209>).
9. Preisler, A. and Brychta, M., "High potential of full year operation with solar driven desiccant evaporative cooling systems", *Energy Procedia*,